inorganics

MDPI

Article

Synthesis and X-ray Structure Analysis of the Polymeric $[Ag_2(4\text{-Amino-}4H\text{-}1,2,4\text{-triazole})_2(NO_3)]_n(NO_3)_n$ Adduct: Anticancer, and Antimicrobial Applications

Mostafa A. El-Naggar [1,*], Hessa H. Al-Rasheed [2,*], Sarah A. AL-khamis [2], Ayman El-Faham [1], Morsy A. M. Abu-Youssef [1], Matti Haukka [3], Assem Barakat [2], Mona M. Sharaf [4] and Saied M. Soliman [1,*]

[1] Department of Chemistry, Faculty of Science, Alexandria University, P.O. Box 426, Ibrahimia, Alexandria 21321, Egypt; ayman.elfaham@alexu.edu.eg (A.E.-F.); morsy5@alexu.edu.eg (M.A.M.A.-Y.)
[2] Department of Chemistry, College of Science, King Saud University, P.O. Box 2455, Riyadh 11451, Saudi Arabia; 441203438@student.ksu.edu.sa (S.A.A.-k.); ambarakat@ksu.edu.sa (A.B.)
[3] Department of Chemistry, University of Jyväskylä, P.O. Box 35, FI-40014 Jyväskylä, Finland; matti.o.haukka@jyu.fi
[4] Protein Research Department, Genetic Engineering and Biotechnology Research Institute, City of Scientific Research and Technological Applications, Alexandria P.O. Box 21933, Egypt
* Correspondence: mostafa.elnaggar@alexu.edu.eg (M.A.E.-N.); halbahli@ksu.edu.sa (H.H.A.-R.); saied1soliman@yahoo.com (S.M.S.)

Abstract: A new Ag(I) adduct was synthesized by the reaction of 4-amino-4*H*-1,2,4-triazole (**L**) with $AgNO_3$. Its chemical structure was approved to be $[Ag_2(L)_2(NO_3)]_n(NO_3)_n$ utilizing elemental analysis, FTIR spectra, and single crystal X-ray diffraction (SC-XRD). According to SC-XRD, there are two independent silver atoms which are coordinated differently depending on whether the nitrate anion is coordinated or not. The coordination geometry of Ag1 is a slightly bent configuration while Ag2 has a distorted tetrahedral structure. The 4-amino-4*H*-1,2,4-triazole ligand and one of the nitrate groups adopt bridging mode, which connects the crystallographically independent Ag1 and Ag2 atoms resulting in the formation of two-dimensional coordination polymer. Hirshfeld surface analysis displays that the intermolecular O···H (34.0%), Ag···N (10.6%), H···H (10.4%), Ag···O (9.3%), and N···H (9.0%) contacts are the most abundant interactions. Regarding anticancer activity, the $[Ag_2(L)_2(NO_3)]_n(NO_3)_n$ demonstrates stronger cytotoxic efficacy against lung (IC_{50} = 3.50 ± 0.37 μg/mL) and breast (IC_{50} = 2.98 ± 0.26 μg/mL) carcinoma cell lines than the anticancer medication *cis*-platin. The $[Ag_2(L)_2(NO_3)]_n(NO_3)_n$ complex showed interesting antibacterial and antifungal activities compared to the free components ($AgNO_3$ and 4-amino-4*H*-1,2,4-triazole). The investigated silver(I) complex exhibits remarkable antibacterial activity against *E. coli* (MIC = 6.1 μg/mL) that may be on par with Gentamycin (MIC = 4.8 μg/mL). As a result, the newly synthesized Ag(I) complex could be suggested for anticancer and antibacterial treatments.

Keywords: Ag(I); 1,2,4-triazole; coordination polymer; Hirshfeld; anticancer; antimicrobial

Citation: El-Naggar, M.A.; Al-Rasheed, H.H.; AL-khamis, S.A.; El-Faham, A.; Abu-Youssef, M.A.M.; Haukka, M.; Barakat, A.; Sharaf, M.M.; Soliman, S.M. Synthesis and X-ray Structure Analysis of the Polymeric $[Ag_2(4\text{-Amino-}4H\text{-}1,2,4\text{-triazole})_2(NO_3)]_n(NO_3)_n$ Adduct: Anticancer, and Antimicrobial Applications. *Inorganics* **2023**, *11*, 395. https://doi.org/10.3390/inorganics11100395

Academic Editor: Ana Maria Da Costa Ferreira

Received: 18 September 2023
Revised: 2 October 2023
Accepted: 6 October 2023
Published: 9 October 2023

1. Introduction

The coordination chemistry of physiologically and pharmacologically active silver(I) compounds is a subject of extensive research, where several silver(I) complexes have been demonstrated as excellent anticancer, antibacterial, or anti-inflammatory substances [1–10]. In particular, it is generally recognized that Ag(I) either in the form of silver salts or coordination compounds, could be used medicinally to treat microbial infections resulting from chronic burns or serious wounds [11–15]. The interaction of the Ag(I) ion with the cell membrane, its ability to make enzyme inactivation, contact with DNA, and disturb the electron transport chain are some of the suggested mechanisms for the biological actions of Ag(I) complexes [16–19]. The type of atoms coordinated to the Ag center, and the possibility of ligand substitutions, have a great impact on the antimicrobial capabilities

of silver complexes. Ag(I) complexes having a higher potential for ligand replacement by physiologically active ligands (sulfur compounds) have more potent antimicrobial effects. As a result, complexes with weak Ag-N and Ag-O bonded species showed a wider range of antimicrobial ability than complexes containing the more stable Ag-S and Ag-P bonds [7,9,10,20,21]. Therefore, it is essential to look for new and superior metal-based compounds as antimicrobial agents. This mission is important especially when considering the rise in antibiotic-resistant bacteria and the difficulty in treating infections [22].

A significant group of heterocyclic compounds is known as triazoles, which have three nitrogen atoms arranged in a five-membered ring. These are classified as 1,2,3- or 1,2,4-triazoles based on the relative positions of the nitrogen atoms in the heterocyclic ring. Because of their wide variety of applications in agrochemicals, medicine, and material sciences, the 1,2,4-triazole nucleus has piqued the interest of researchers. The 1,2,4-triazole nucleus is resistant to metabolic degradation and exhibits target selectivity as well as a broad spectrum of activity. In addition, this nucleus can also coordinate with a variety of metal ions to generate organometallic compounds with diverse biological functions [23]. Several substituted 1,2,4-triazole compounds were reported to have interesting bioactivity as antimicrobial, antifungal [24], anti-tubercular [25], anti-inflammatory [26], antidiabetic [27], hypoglycaemic [28], anticonvulsant [29], antidepressant [30], anti-malarial [31], arthritis [32], anti-migraine [33], antiviral [34], antihypertensive [35,36], potassium channel activators [37], antileishmanial [38], antioxidant [39], and antiplatelet [40].

In this article, we reported the synthesis and characterization of a new silver(I) complex constructed from 4-amino-4*H*-1,2,4-triazole (**L**) (Figure 1) and $AgNO_3$. The bioactive ligand 4-amino-4*H*-1,2,4-triazole would work in concert with the Ag(I) ion to provide an effective antimicrobial and anticancer material. In this regard, the in vitro antimicrobial and anticancer activities of the new Ag(I) complex were reported and compared with the free components, 4-amino-4*H*-1,2,4-triazole (**L**) and $AgNO_3$. In addition, the supramolecular structural aspects of the new complex were presented for the first time.

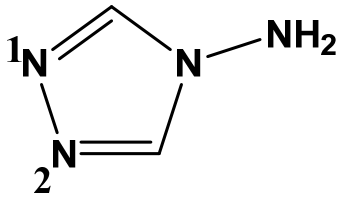

Figure 1. Structural formula of 4-amino-4*H*-1,2,4-triazole (**L**).

2. Results and Discussion

2.1. Synthesis and Characterization

In previous work, the mononuclear adduct $[Ag(L)_2]NO_3$ was reported. Based on the FTIR spectroscopic data, the 4-amino-4*H*-1,2,4-triazole (**L**) is proposed to be a terminal N-donor ligand via N1 atom [41]. It was reported by authors that, the adduct $[Ag(L)_2]NO_3$ was obtained by mixing $AgNO_3$ and 4-amino-4*H*-1,2,4-triazole in ratio of 1:3. It is worthy of note that there no X-ray single crystal structure characterization was reported for this complex. On the other hand, the $[Ag(L)_{1.75}]_n(NO_3)_n$ and $[Ag(L)_{1.25}](NO_3)$ complexes were obtained by mixing equimolar amounts of $AgNO_3$ and 4-amino-4*H*-1,2,4-triazole in 3 mL of MeCN [42]. The structure of $[Ag(L)_{1.75}]_n(NO_3)_n$ was confirmed with no doubt by X-ray diffraction of single crystal. In our work, we reported the synthesis of a new polymeric silver(I) complex of the same ligand in which the Ag:**L** ratio is 1:1. The new complex was obtained by mixing ethanolic solution of **L** with an aqueous solution of $AgNO_3$ then the resulting white precipitate was in situ dissolved in MeCN (Scheme 1). After a couple of days, colorless crystals suitable for single crystal X-ray diffraction were obtained. This procedure developed a new supramolecular crystalline complex that exists as two-dimensional polymeric chains exploited by the bridging ligand groups, which act as linkers between silver sites.

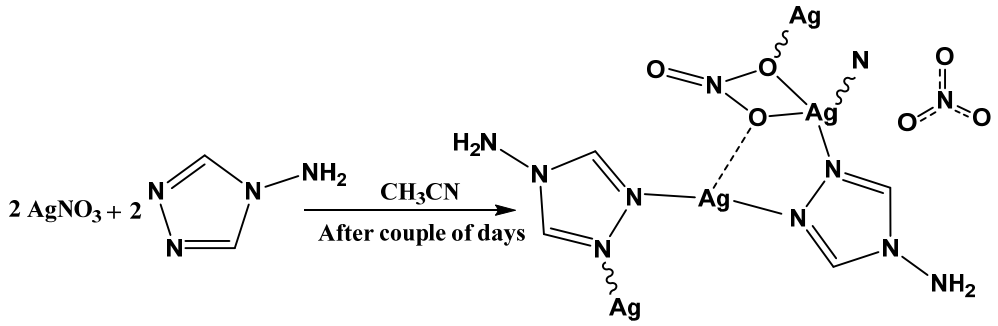

Scheme 1. Synthesis of $[Ag_2(L)_2(NO_3)]_n(NO_3)_n$.

2.2. X-ray Crystal Structure of $[Ag_2(L)_2(NO_3)]_n(NO_3)_n$

Single-crystal X-ray structural study showed that the $[Ag_2(L)_2(NO_3)]_n(NO_3)_n$ complex crystallizes in the orthorhombic crystal system and the *Pccn* space group with $Z = 8$. The crystal information is displayed in Table S1, Supplementary Materials. The unit cell parameters are a = 6.97690(10) Å, b = 12.90670(10) Å and c = 27.7850(2) Å, while the unit cell volume is 2502.00(4) Å^3. Figure 2 shows the atom numbering and coordination geometry of the $[Ag_2(L)_2(NO_3)]_n(NO_3)_n$ complex. There are two silver ions, two organic ligands, and two nitrate anions in the asymmetric unit (Figure 2). In the literature, the bridging mode of 1,2,4-triazoles via N1 and N2 (Figure 1) is well acknowledged and appears to be a general feature [42–44]. In addition, Ag(I) is an extremely soft Lewis acid and it has a flexible and versatile coordination sphere that can accommodate a wide range of stable coordination numbers between 2 and 6 [45]. As a result, Ag(I) can establish linear [46,47], trigonal [48], tetrahedral [49,50], square-planar [51], trigonal pyramidal [52,53], T-shaped [54] or octahedral coordination geometries [55]. This variety in the coordination sphere of silver(I) is due in part to the lack of stereochemical preference for the d^{10} electronic configuration. In this context, the compound under study has two crystallographically independent silver atoms that are differently coordinated depending on whether the nitrate group is coordinated or not. The Ag1 is coordinated by N4 and N5 of two triazole moieties, forming a slightly bent geometry where the N4–Ag1–N5 angle is 171.52(4)°. The two coordinating triazole systems are not co-planar because the angle between their ring mean planes is 41.54°. Also, these 4-substituted triazole rings are in anti-configuration to one another. On the other hand, Ag2 has a distorted tetrahedral geometry where the Ag2 center is coordinated with two N-atoms from two triazole ligand units that occupy syn-configuration to one another, in addition to two oxygen atoms (O1 and O2) belonging to a bidentate nitrate group. In this case, the two triazole ligand units are coordinated to the central Ag2 atom through the nitrogen atoms N3 and N8, where the Ag–N distances are 2.2087(9) and 2.2184(9) Å, respectively. Also, the two Ag2–O1 (2.5044(9) Å) and Ag2–O2 (2.5202(9) Å) bonds are nearly equidistant. It is clear that the two coordinating triazole systems around the Ag2 center are nearly co-planar, where the angle between their mean planes is only 10.83°. Table 1 displays selected interatomic distances and bond angles.

Table 1. Bond lengths [Å] and angles [°] for $[Ag_2(L)_2(NO_3)]_n(NO_3)_n$.

Bond	Distance	Bond	Distance
Ag(1)–N(4)	2.1375(9)	Ag(2)–N(8)	2.2184(9)
Ag(1)–N(5)	2.1407(9)	Ag(2)–O(1)	2.5044(9)
Ag(2)–N(3)#1	2.2087(9)	Ag(2)–O(2)	2.5202(9)
Bonds	**Angle**	**Bonds**	**Angle**
N(4)–Ag(1)–N(5)	171.52(4)	N(3)#1–Ag(2)–O(2)	127.71(3)
N(3)#1–Ag(2)–N(8)	132.98(3)	N(8)–Ag(2)–O(2)	95.06(3)
N(3)#1–Ag(2)–O(1)	100.41(3)	O(1)–Ag(2)–O(2)	51.31(3)
N(8)–Ag(2)–O(1)	123.76(3)		

#1: −x, y + 1/2, −z + 1/2.

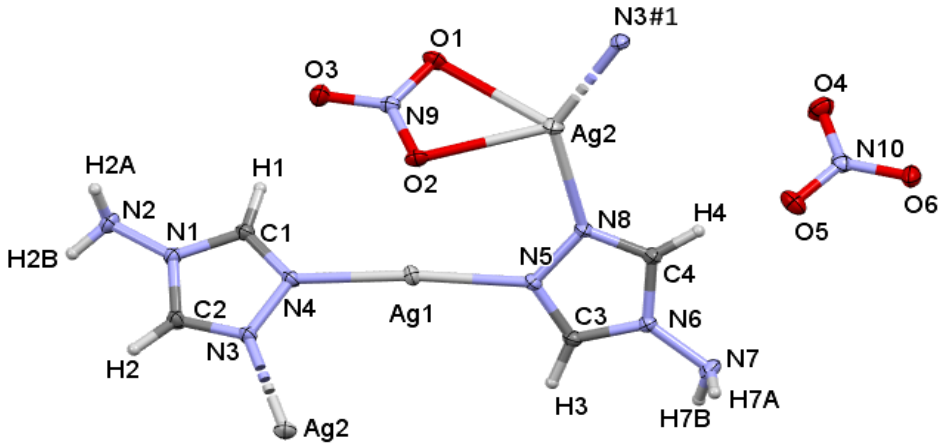

Figure 2. X-ray structure of $[Ag_2(L)_2(NO_3)]_n(NO_3)_n$, symmetry code to generate N3#1 is −x, y + 1/2, −z + 1/2.

The two Ag(1) and Ag(2) centers are bridged to one another via the two neighboring N-atoms of the 1,2,4-triazole ring, which leads to a wavy-like coordination polymer extending the along the *b*-direction (Figure 3). However, the Ag1–O2 and Ag1–O1#1 (#1 = 0.5 − x, 1.5 − y, z) bond lengths are determined to be 2.749(1) and 2.765(1) Å, which are close to 2.75 Å. Hence, both of the 1,2,4-triazole ligand units and one of the nitrate groups, which has lower atom numbering, adopt bridging modes, giving rise to the formation of two-dimensional coordination polymer (Figure 3).

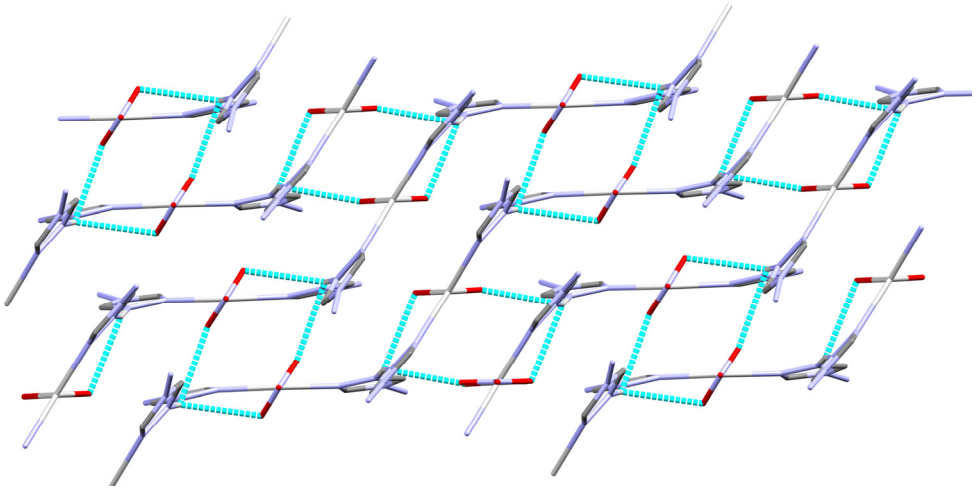

Figure 3. The projections of the polymer chains showing the wavy-like pattern along *b*-direction and the two-dimensional infinite coordination polymer of the $[Ag_2(L)_2(NO_3)]_n(NO_3)_n$ complex. The weak Ag1–O2 and Ag1–O1#1 (#1 = 1/2 − x, 1/2 − y, z) bonds are presented by dotted turquoise line. All hydrogen atoms were omitted from this figure for better visualization.

It is clear from the reported X-ray structure that the amino group is not included in the coordination environment of any of the two Ag atoms. On the other hand, the amino groups are included in the supramolecular structure of the $[Ag_2(L)_2(NO_3)]_n(NO_3)_n$ complex as hydrogen bond donor, while the nitrate ions are the hydrogen bond acceptors. Hence, the 3D crystalline structure of the $[Ag_2(L)_2(NO_3)]_n(NO_3)_n$ complex is stabilized by many polar intermolecular N–H···O hydrogen bonds shown in Figure 4, while Table 2 shows the respective hydrogen bond parameters. Particularly, the uncoordinated nitrate group contributed greatly to the molecular packing via all of its oxygen atoms (O4, O5, and O6) leading to the formation of strong N–H···O hydrogen bonds with the free amino groups. The H2A and H2B of the amino group connect the O4 and O5 of the nitrate group with hydrogen to acceptor distances of 2.12(2) and 2.281(19) Å, respectively. Also, the N–H

protons H7A and H7B from the other amino group, as hydrogen bond donors, form two N–H···O hydrogen bonds with O6 from the same nitrate counter-ion as the hydrogen bond acceptor (Figure 4a). In addition, some non-classical C–H···O interactions are observed in the supramolecular structure of the investigated complex, which occur between the atom O3 of the coordinated nitrate group with H1 and H3 atoms from the triazole moiety (Table 2). Also, the O4 and O5 atoms of the ionic nitrate form weak C–H···O interactions with H2 and H4 atoms of the triazole unit. The H···O distances are 2.34 and 2.29 Å, respectively. As shown in Figure 4b, the $[Ag_2(L)_2(NO_3)]_n(NO_3)_n$ coordination polymer chains are cross-linked by strong N–H···O hydrogen bonds and weak C–H···O interactions to give a 3D supramolecular network.

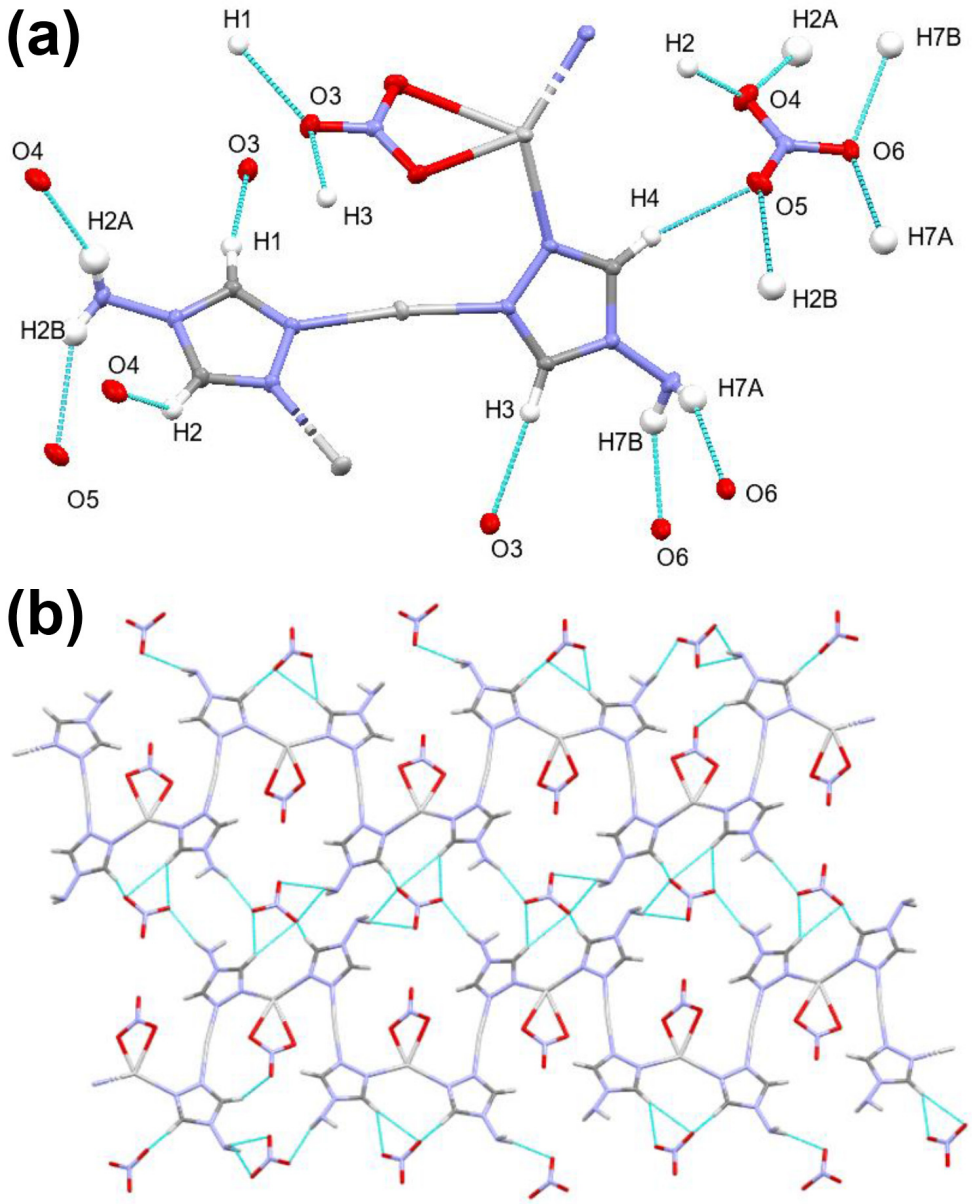

Figure 4. Hydrogen bonds in $[Ag_2(L)_2(NO_3)]_n(NO_3)_n$ represented by red dotted lines (**a**), and the crystal packing of the polymeric chains via hydrogen bonding interactions (**b**).

Table 2. Hydrogen bonds for $[Ag_2(L)_2(NO_3)]_n(NO_3)_n$ [Å and °].

D–H···A	d(D–H)	d(H···A)	d(D···A)	<(DHA)
C(2)–H(2)···O(4)#1	0.95	2.34	3.0520(15)	131.2
N(2)–H(2A)···O(4)#2	0.85(2)	2.12(2)	2.9308(15)	160.5(19)
N(2)–H(2B)···O(5)#3	0.876(19)	2.281(19)	3.0142(14)	141.2(17)
C(3)–H(3)···O(3)#3	0.95	2.36	3.2420(13)	154.7
N(7)–H(7A)···O(6)#4	0.828(19)	2.301(19)	3.0714(15)	154.9(17)
N(7)–H(7B)···O(6)#5	0.878(19)	2.119(19)	2.9295(14)	153.1(16)
C(1)–H(1)···O(3)#6	0.95	2.4	3.3135(14)	160.3
C(4)–H(4)···O(5)	0.95	2.29	3.1399(14)	147.9

Symmetry codes: #1: −x, y − 1/2, −z + ½; #2: x, −y + 3/2, z − 1/2; #3: x + 1/2, −y + 1, −z + ½; #4: −x, −y + 1, −z + 1; #5: x + 1/2, y − 1/2, −z + 1; #6: −x + 1/2, −y + 3/2, z.

The X-ray structure of $[Ag_2(L)_2(NO_3)]_n(NO_3)_n$ is significantly different from that of the previously reported complex $[Ag(L)_{1.75}]_n(NO_3)_n$. The latter crystallized in the monoclinic crystal system and C2/c space group with Z = 8. Also, the asymmetric unit consists of two different Ag(I) cations, three whole and one-half of **L**, and two uncoordinated NO_3^- anions. Also, it consists of two crystallographically independent silver atoms; the Ag1 atom has triangular planar coordination geometry, while Ag2 is tetrahedrally coordinated. Unlike Ag2 in $[Ag_2(L)_2(NO_3)]_n(NO_3)_n$, the Ag2 in $[Ag(L)_{1.75}]_n(NO_3)_n$ is coordinated by triazole rings only, whereas all the nitrate anions are freely uncoordinated. In both complexes, the 4-amino-4*H*-1,2,4-triazole acts as μ_2-N1,N2 bridging ligand without any participation for the amino group in the coordination environment [42].

2.3. FTIR Spectra

The IR spectral analyses of the complex $[Ag_2(L)_2(NO_3)]_n(NO_3)_n$ and its free organic ligand, 4-amino-4*H*-1,2,4-triazole, have been recorded and presented in Figures S1 and S2 (Supplementary Materials). The FTIR spectrum of the complex differs slightly from that of the free ligand. For the $[Ag_2(L)_2(NO_3)]_n(NO_3)_n$ complex, the appearance of a sharp, prominent peak at 1383 cm^{-1} points to the existence of the nitrate group, which is absent in the spectrum of the free organic ligand. In the spectrum of the free ligand, the band at 1635 cm^{-1} could be assigned to the ν(C=N) stretching mode of the triazole ring. It is slightly shifted to lower wavenumber of 1631 cm^{-1} in case of the $[Ag_2(L)_2(NO_3)]_n(NO_3)_n$ complex. The observed change in the shape and the slight shift in the band position of the ν(C=N) mode in the FTIR spectrum of the $[Ag_2(L)_2(NO_3)]_n(NO_3)_n$ complex demonstrates the coordination of **L** with the silver ion. In the spectra of the complex and its free ligand, the bands appearing at 3130 cm^{-1} could be attributed to the C(sp^2)-H stretching vibrations of the triazole ring. Furthermore, there are strong absorption peaks at 3201–3203 cm^{-1} and 3302–3321 cm^{-1} corresponding to $\upsilon(NH_2)$.

2.4. Analysis of Molecular Packing

It is generally known that the molecules in the crystals are packed through intermolecular interactions, which enhance the crystal's stability. Hirshfeld surface calculations gave a full description of the supramolecular structure of crystalline materials. Hence, it presents a better understanding of the molecular packing even for weak interactions, which are hard to detect but are critical for crystal packing. The contributions of all possible intermolecular contacts in the $[Ag_2(L)_2(NO_3)]_n(NO_3)_n$ complex are estimated using fingerprint plots and reported in Figure 5. As expected, the O···H (34.0%) contacts are the most important in the supramolecular structure of the $[Ag_2(L)_2(NO_3)]_n(NO_3)_n$ complex. Additionally, Ag···N (10.6%), H···H (10.4%), Ag···O (9.3%), and N···H (9.0%) contacts contributed significantly to the molecular packing.

The different Hirshfeld surfaces (d_{norm}, curvedness, and shape index) of the asymmetric $[Ag_2(L)_2(NO_3)](NO_3)$ unit are shown in Figure 6. In the upper part of this figure, the d_{norm} maps reveal the presence of numerous red spots attributed to the significant intermolecular interactions. The small percentage of C···C interactions (1.0%) and the

absence of blue/red triangles in the shape index map pointed out to the absence of π–π stacking interactions.

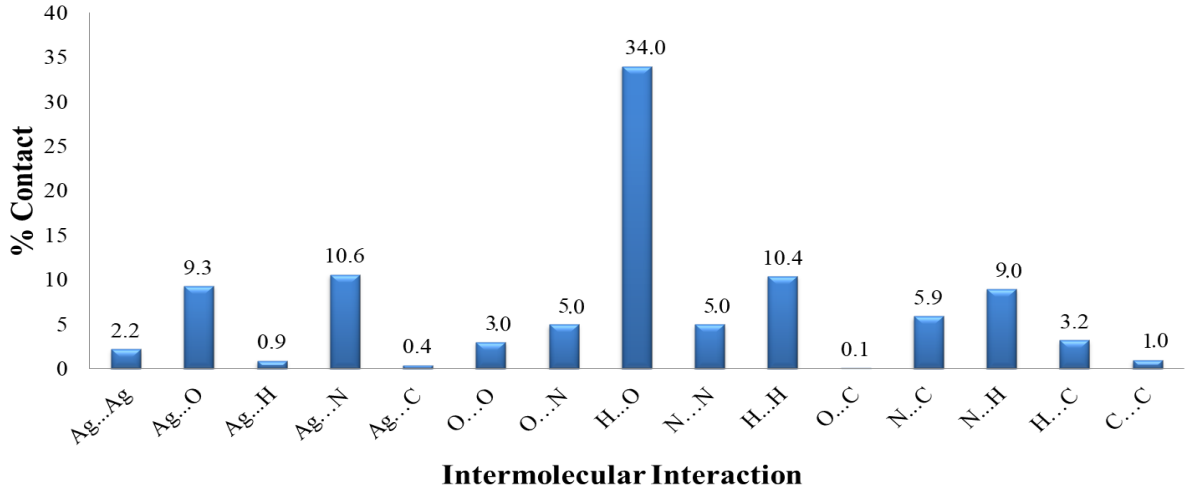

Figure 5. Percentages of all intermolecular contacts in the $[Ag_2(L)_2(NO_3)]_n(NO_3)_n$ complex.

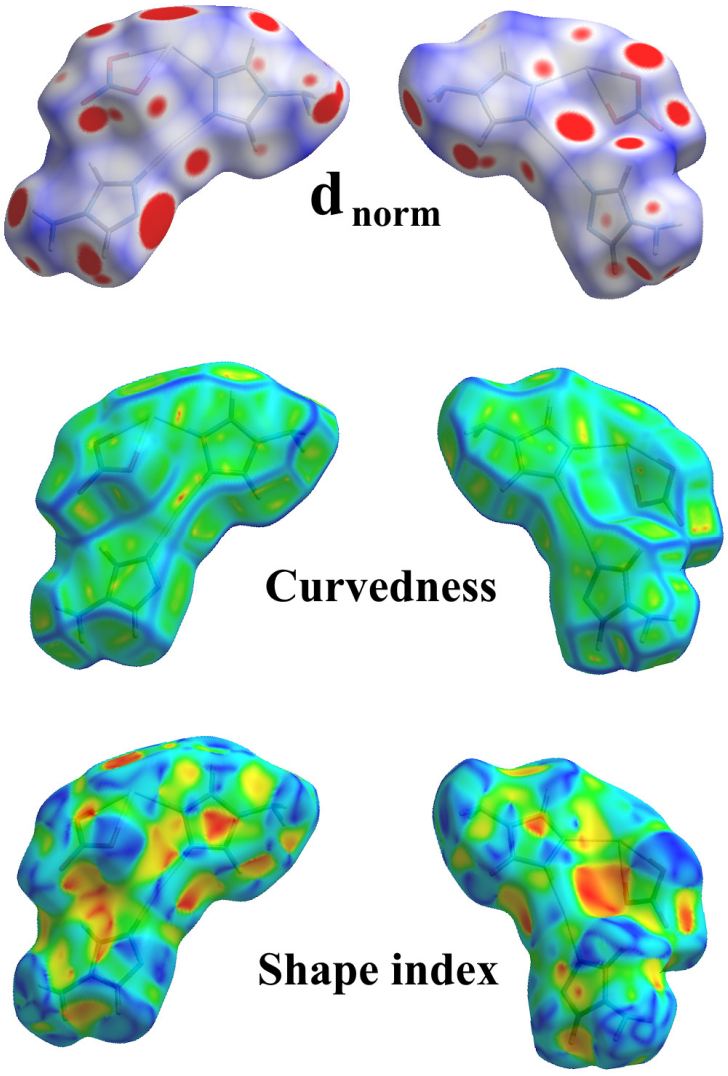

Figure 6. Hirshfeld surfaces for the asymmetric $[Ag_2(L)_2(NO_3)](NO_3)$ unit.

The significance of O···H and N···H contacts in the supramolecular structure of $[Ag_2(L)_2(NO_3)]_n(NO_3)_n$ complex is evident from Figure 7, since their d_{norm} surfaces and fingerprint (FP) plots showed intense red spots and sharp spikes, respectively (Figure 7).

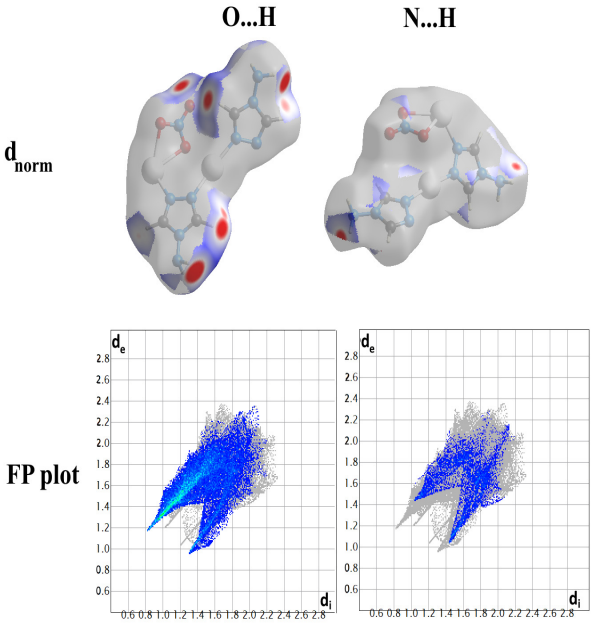

Figure 7. The d_{norm} maps and fingerprint plots of the O···H and N···H contacts.

The packing is also dominated by numerous Ag–N coordination interactions (10.6%), which are involved in the polymeric structure of $[Ag_2(L)_2(NO_3)](NO_3)$ via the bridging triazole ligand. Additionally, Ag–O interactions contributed to the packing by 9.3%. All Ag–N and Ag–O interactions are manifested as red spots in the corresponding d_{norm} maps and strong spikes in fingerprint plots, as shown in Figure 8.

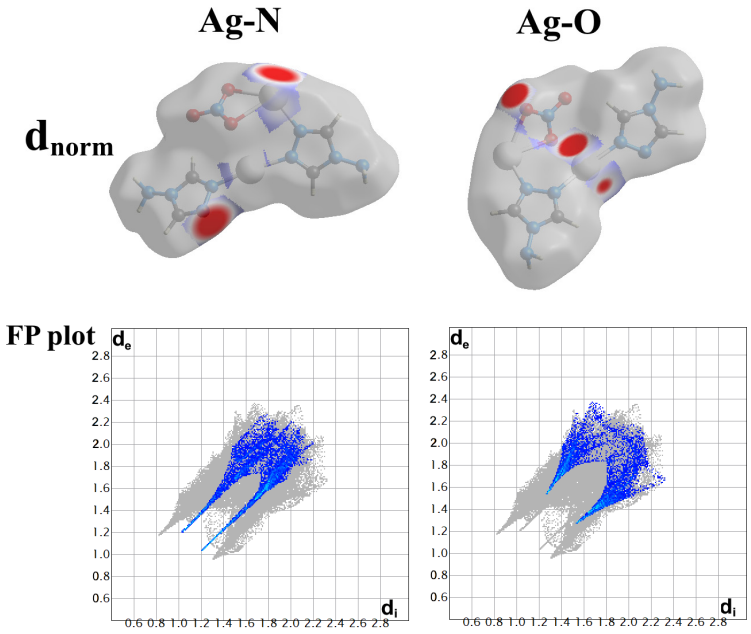

Figure 8. The d_{norm} maps and fingerprint plots of the Ag-N and Ag-O interactions.

As shown in Figure 9, there are some Ag···Ag interactions (2.2%) among the polymeric chains since the Ag···Ag distance equals 3.516 Å, which means the presence of some argentophillic interaction [56]. Also, nitrogen atoms from the amino, nitrate, and triazole

groups have an important role in the packing through C···N, N···N, and N···O contacts. Their percentages are 5.9, 5.0, and 5.0%, respectively (Figure S3).

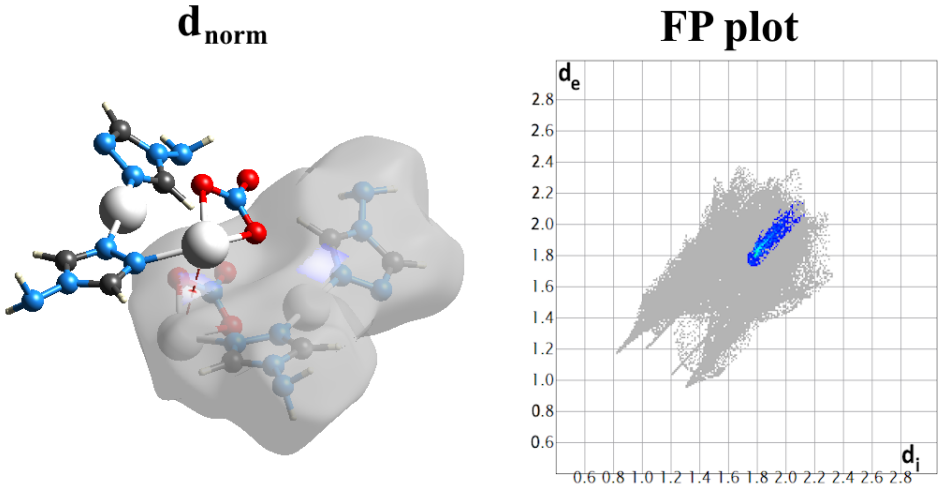

Figure 9. The d_{norm} map and fingerprint plot of the Ag···Ag contact.

2.5. Cytotoxic Activity

The MTT methodology was applied to evaluate the in vitro cytotoxicity of the $[Ag_2(L)_2(NO_3)]_n(NO_3)_n$ complex as IC_{50} values in μg/mL towards two human tumor cell lines, lung (A-549) and breast (MCF-7) carcinoma. The comprehensive outcomes are included in Tables S2–S5 (Supplementary Materials) and visually shown in Figure S4. A summary of these results is provided in Table 3. The cytotoxic potential of the $[Ag_2(L)_2(NO_3)]_n(NO_3)_n$ complex is compared to that of the free L and $AgNO_3$ as well. The $[Ag_2(L)_2(NO_3)]_n(NO_3)_n$ complex exhibited greater potency and lower IC_{50} values than the free ligand against the two cell lines (Table 3). In comparison with $AgNO_3$, the $[Ag_2(L)_2(NO_3)]_n(NO_3)_n$ complex displays better cytotoxicity in case of lung carcinoma while both $AgNO_3$ (2.81 ± 0.97 μg/mL) and $[Ag_2(L)_2(NO_3)]_n(NO_3)_n$ (2.98 ± 0.26 μg/mL) complex have comparable cytotoxicity against breast carcinoma.

Table 3. IC_{50} values (in μg/mL) for $[Ag_2(L)_2(NO_3)]_n(NO_3)_n$, free **L**, $AgNO_3$ and *cis*-platin against selected cancer cell lines.

Compound	A-549	MCF-7
$[Ag_2(L)_2(NO_3)]_n(NO_3)_n$	3.50 ± 0.37	2.98 ± 0.26
L	366.99 ± 13.94	270.39 ± 11.86
$AgNO_3$	14.70 ± 0.53	2.81 ± 0.97
cis-Platin	7.5 ± 0.69	4.59 ± 0.53

cis-platin is a powerful, well-known anticancer medication which is still currently in use [57], in spite of its undesirable side effects [58–60]. Ag(I) complexes have gained some popularity as candidates for cancer treatments with little side effects on healthy human cells [3–5,8,61–65]. In comparison to *cis*-platin and under the same experimental conditions, the new complex $[Ag_2(L)_2(NO_3)]_n(NO_3)_n$ has a higher cytotoxic potential towards lung and breast cancer cell lines since the IC_{50} values of the studied complex are about half of those of *cis*-platin for both cell lines (Table 3).

2.6. Antimicrobial Activity

Ag(I) complexes based on various *N*-heterocycles exhibited fascinating antimicrobial properties [2,10,66,67]. In this regard, the antimicrobial characteristics of the $[Ag_2(L)_2(NO_3)]_n(NO_3)_n$ complex were assessed as minimum inhibition concentrations (MIC) and inhibition zone diameters towards six pathogens. The results have been compared with those of other

commercially available antibiotics such as Gentamycin and Ketoconazole as antibacterial and antifungal positive controls, respectively (Tables 4 and S6 (Supplementary Materials)). The free ligand has no antimicrobial activity towards all tested microbes. On the contrary, the $[Ag_2(L)_2(NO_3)]_n(NO_3)_n$ has wide-spectrum action against all examined microorganisms except *A. fumigatus*. This shed the light on how biological activity is boosted when Ag(I) is coordinated. Interestingly, the investigated silver (I) complex displays excellent antibacterial activity towards *E. coli* (MIC = 6.1 µg/mL), which could be comparable to Gentamycin (MIC = 4.8 µg/mL). On the other hand, the Ag(I) complex, $AgNO_3$, and the free organic ligand, all have no antifungal activity against *A. fumigatus* at the applied concentration. It is well known that the higher the activity of the complex, the larger the diameters of the inhibition zones and the smaller the MIC values (Tables 4 and S6 (Supplementary Materials)).

Table 4. The MIC (µg/mL) values for $[Ag_2(L)_2(NO_3)]_n(NO_3)_n$, free **L**, $AgNO_3$, and positive controls.

Compound	Gram-Positive Bacteria		Gram-Negatvie Bacteria		Fungi	
	S. aureus	*B. subtilis*	*E. coli*	*P. vulgaris*	*A. fumigatus*	*C. albicans*
$[Ag_2(L)_2(NO_3)]_n(NO_3)_n$.	30.5	64	6.1	32	ND	156
$AgNO_3$	64	312.5	32	156	ND	128
L	ND	ND	ND	ND	ND	ND
Control	9.7 [a]	4.8 [a]	4.8 [a]	4.8 [a]	156.25 [b]	312.5 [b]

[a] Gentamycin; [b] Ketoconazole; ND: Not determined.

3. Materials and Methods

3.1. Chemicals and Physicochemical Characterizations

All the chemicals were obtained from Sigma-Aldrich Company (Burlington, MA, USA). The FTIR spectral analysis was conducted at 4000–400 cm^{-1} by a Bruker Tensor 37 FTIR instrument (Bruker Company, Karlsruhe, Germany) in KBr pellets. The CHN elemental analysis was performed by a Perkin Elmer 2400 Elemental Analyzer (PerkinElmer, New York, NY, USA). A Shimadzu atomic absorption spectrophotometer (AA-7000 series, Shimadzu, Ltd., Kyoto, Japan) was used to measure the quantity of Ag.

3.2. Synthesis of $[Ag_2(L)_2(NO_3)]_n(NO_3)_n$

A 10 mL aqueous solution of silver nitrate (84.9 mg, 0.5 mmol) was mixed with a solution of 4-amino-4*H*-1,2,4-triazole (42.0 mg, 0.5 mmol) in ethanol at room temperature. This mixture gives rise to the formation of a precipitate which then dissolved in acetonitrile. The resulting solution was kept at room temperature and allowed to evaporate slowly. The complex $[Ag_2(L)_2(NO_3)]_n(NO_3)_n$ was obtained as colorless crystals within a few days. The crystals obtained were appropriate for single crystal X-ray measurements.

$[Ag_2(L)_2(NO_3)]_n(NO_3)_n$; (77% yield). Anal. Calc. $C_4H_8Ag_2N_{10}O_6$: C, 9.46; H, 1.59; N, 27.58; Ag, 42.48%. Found: C, 9.50; H, 1.56; N, 27.49; Ag, 42.61%. FTIR cm^{-1}: 3436, 3302, 3201, 3130, 1631, 1528, 1383, 1197, 1073, 982, 865, 825, 619. **L**: 3411, 3321, 3203, 3130, 1635, 1527, 1196, 1073, 979, 864, 620 (Figures S1 and S2, Supplementary Materials).

3.3. Crystal Structure Analysis

X-ray structural analysis and instrument details are illustrated in the Supplementary Materials [68–71]. Table S1 displays the crystal information for the $[Ag_2(L)_2(NO_3)]_n(NO_3)_n$ complex.

3.4. Hirshfeld Surface Analysis

The 2D fingerprint plots and Hirshfeld surfaces were generated using the Crystal Explorer Ver. 3.1 software program [72].

3.5. Determination of Cytotoxic and Antimicrobial Activities

The technique described in Method S1 (Supplementary Materials) was used to assess the cytotoxic effectiveness of the $[Ag_2(L)_2(NO_3)]_n(NO_3)_n$ complex against lung (A-549) and breast (MCF-7) cancer cell lines (American Type Culture Collection (ATCC, Rockville, MD, USA)) [73]. Gram-positive bacteria, Gram-negative bacteria, and harmful yeasts were used for testing the antimicrobial potency of the Ag(I) complex, $AgNO_3$ and its free ligand. More details can be found in Method S2 (Supplementary Materials).

4. Conclusions

In this work, the structure of the polymeric $[Ag_2(L)_2(NO_3)]_n(NO_3)_n$ complex was discussed based on the X-ray single crystal diffraction analysis. There are two crystallographically independent silver centers which are differently coordinated. Ag1 has a slightly bent AgN_2 coordination environment while Ag2 has strongly distorted AgN_2O_2 coordination geometry. The 1D polymer grows via the bridging triazole ligand. Hirshfeld analysis was used to perform qualitative and quantitative analyses of the supramolecular architecture of the $[Ag_2(L)_2(NO_3)]_n(NO_3)_n$ complex. The most crucial contact is the O···H interaction (34%). Biological investigations showed the excellent antimicrobial and anticancer properties of the $[Ag_2(L)_2(NO_3)]_n(NO_3)_n$ complex. Depending on inhibition zone diameters and MIC values, the Ag(I) complex has interesting potential towards Gram-negative bacteria, Gram-positive bacteria, and fungi, whereas the free ligand 4-amino-4*H*-1,2,4-triazole (**L**) showed no activity against all examined microbes. The anticancer activities of the silver(I) complex are higher than those of the triazole ligand and the anticancer drug *cis*-platin against lung and breast cancer cell lines. As a result, we are inspired to conduct additional research on this interesting group of Ag(I) compounds, which have attractive prospects for antitumor characteristics.

Supplementary Materials: The following supporting information can be downloaded at: https://www.mdpi.com/article/10.3390/inorganics11100395/s1, Figure S1: FTIR spectrum of the free ligand; Table S1: Crystallographic details and crystal refinement parameters for the complex $[Ag_2(L)_2(NO_3)]_n(NO_3)_n$; FTIR spectrum of the free ligand; Figure S2: FTIR spectrum of the complex; $[Ag_2(L)_2(NO_3)]_n(NO_3)_n$; Figure S3. d_{norm} maps of C···N, N···N, and N···O contacts. The C···N contacts occur between the parallel triazole rings, N···N interactions occurred between amino groups while N···O contacts occur between the nitrate groups; Figure S4. The anticancer action of the studied complex, free ligand and $AgNO_3$ against A-549 lung (upper) and MCF-7 breast (lower) carcinoma cells lines; Table S2: Evaluation of cytotoxicity against the A-549 cell line for the free ligand; Table S3: Evaluation of cytotoxicity against the A-549 cell line for the complex $[Ag_2(L)_2(NO_3)]_n(NO_3)_n$; Table S4: Evaluation of cytotoxicity against the MCF-7 cell line for the free ligand; Table S5: Evaluation of cytotoxicity against the MCF-7 cell line for $[Ag_2(L)_2(NO_3)]_n(NO_3)_n$; Table S6: Inhibition zone diameters (mm) for $[Ag_2(L)_2(NO_3)]_n(NO_3)_n$, free L, $AgNO_3$, and positive controls; Method S1: Evaluation of cytotoxic effects against the two human lung (A-549) and breast (MCF-7) cancer cell lines; Method S2: Testing of antimicrobial activity.

Author Contributions: Conceptualization, M.A.M.A.-Y. and S.M.S.; methodology, M.A.E.-N.; software, M.H. and S.M.S.; validation, M.A.E.-N., A.B. and S.M.S.; formal analysis, M.A.E.-N. and M.H.; investigation, M.A.E.-N.; resources, A.B., A.E-F., H.H.A.-R., S.A.A.-k. and S.M.S.; data curation, S.M.S. writing—original draft preparation, M.A.E.-N., M.A.M.A.-Y., A.B., A.E.-F., H.H.A.-R., S.A.A.-k., M.H., M.M.S. and S.M.S.; writing—review and editing, M.A.E.-N., M.A.M.A.-Y., M.H., A.B. and S.M.S.; supervision, M.A.M.A.-Y. and S.M.S.; project administration, A.B., A.E.-F., H.H.A.-R., S.A.A.-k. and S.M.S.; funding acquisition, A.B. All authors have read and agreed to the published version of the manuscript.

Funding: The Deputyship for Research and Innovation, "Ministry of Education", King Saud University (IFKSUOR3-188-4), Saudi Arabia.

Data Availability Statement: Data is contained within the paper.

Acknowledgments: The authors extend their appreciation to the Deputyship for Research and Innovation, "Ministry of Education" in Saudi Arabia for funding this research (IFKSUOR3-188-4).

Conflicts of Interest: The authors declare no conflict of interest.

References

1. El-Naggar, M.A.; Sharaf, M.M.; Albering, J.H.; Abu-Youssef, M.A.M.; Kassem, T.S.; Soliman, S.M.; Badr, A.M.A. One Pot Synthesis of Two Potent Ag(I) Complexes with Quinoxaline Ligand, X-Ray Structure, Hirshfeld Analysis, Antimicrobial, and Antitumor Investigations. *Sci. Rep.* **2022**, *12*, 20881. [CrossRef] [PubMed]
2. El-Naggar, M.A.; Abu-Youssef, M.A.M.; Soliman, S.M.; Haukka, M.; Al-Majid, A.M.; Barakat, A.; Badr, A.M.A. Synthesis, X-Ray Structure, Hirshfeld, and Antimicrobial Studies of New Ag(I) Complexes Based on Pyridine-Type Ligands. *J. Mol. Struct.* **2022**, *1264*, 133210. [CrossRef]
3. Tan, S.J.; Yan, Y.K.; Lee, P.P.F.; Lim, K.H. Copper, Gold and Silver Compounds as Potential New Anti-Tumor Metallodrugs. *Future Med. Chem.* **2010**, *2*, 1591–1608. [CrossRef]
4. Journal of Pharmaceuticals, G.; Kumar Raju, S.; Karunakaran, A.; Kumar, S.; Sekar, P.; Murugesan, M.; Karthikeyan, M. Silver Complexes as Anticancer Agents: A Perspective Review. *Ger. J. Pharm. Biomater.* **2022**, *1*, 6–28.
5. Altowyan, M.S.; El-Naggar, M.A.; Abu-Youssef, M.A.M.; Soliman, S.M.; Haukka, M.; Barakat, A.; Badr, A.M.A. Synthesis, X-Ray Structure, Antimicrobial and Anticancer Activity of a Novel [Ag(Ethyl-3-Quinolate)$_2$(Citrate)] Complex. *Crystals* **2022**, *12*, 356. [CrossRef]
6. Abu-Youssef, M.A.M.; Soliman, S.M.; Langer, V.; Gohar, Y.M.; Hasanen, A.A.; Makhyoun, M.A.; Zaky, A.H.; Öhrström, L.R. Synthesis, Crystal Structure, Quantum Chemical Calculations, DNA Interactions, and Antimicrobial Activity of [Ag(2-Amino-3-Methylpyridine)$_2$]NO_3 and [Ag(Pyridine-2-Carboxaldoxime)NO_3]. *Inorg. Chem.* **2010**, *49*, 9788–9797. [CrossRef]
7. Isab, A.A.; Nawaz, S.; Saleem, M.; Altaf, M.; Monim-ul-Mehboob, M.; Ahmad, S.; Evans, H.S. Synthesis, Characterization and Antimicrobial Studies of Mixed Ligand Silver(I) Complexes of Thioureas and Triphenylphosphine; Crystal Structure of {[Ag(PPh_3)(Thiourea)(NO_3)]$_2$·[Ag(PPh_3)(Thiourea)]$_2$(NO_3)$_2$}. *Polyhedron* **2010**, *29*, 1251–1256. [CrossRef]
8. Tan, X.J.; Liu, H.Z.; Ye, C.Z.; Lou, J.F.; Liu, Y.; Xing, D.X.; Li, S.P.; Liu, S.L.; Song, L.Z. Synthesis, Characterization and in Vitro Cytotoxic Properties of New Silver(I) Complexes of Two Novel Schiff Bases Derived from Thiazole and Pyrazine. *Polyhedron* **2014**, *71*, 119–132. [CrossRef]
9. Nawaz, S.; Isab, A.A.; Merz, K.; Vasylyeva, V.; Metzler-Nolte, N.; Saleem, M.; Ahmad, S. Synthesis, Characterization and Antimicrobial Studies of Mixed Ligand Silver(I) Complexes of Triphenylphosphine and Heterocyclic Thiones: Crystal Structure of Bis[{(M2-Diazinane-2-Thione)(Diazinane-2-Thione)(Triphenylphosphine)Silver(I) Nitrate}]. *Polyhedron* **2011**, *30*, 1502–1506. [CrossRef]
10. Nomiya, K.; Tsuda, K.; Sudoh, T.; Oda, M.; Bongoza, U.; Zamisa, S.J.; Munzeiwa, W.A.; Omondi, B.; Celik, S.; Yurdakul, S.; et al. Ag(I)-N Bond-Containing Compound Showing Wide Spectra in Effective Antimicrobial Activities: Polymeric Silver(I) Imidazolate. *J. Inorg. Biochem.* **1997**, *68*, 39–44. [CrossRef]
11. Mohan, M.; Gupta, S.K.; Kalra, V.K.; Vajpayee, R.B.; Sachdev, M.S. Topical Silver Sulphadiazine--a New Drug for Ocular Keratomycosis. *Br. J. Ophthalmol.* **1988**, *72*, 192–195. [CrossRef] [PubMed]
12. Klasen, H.J. A Historical Review of the Use of Silver in the Treatment of Burns. II. Renewed Interest for Silver. *Burns* **2000**, *26*, 131–138. [CrossRef] [PubMed]
13. De Gracia, C.G. An Open Study Comparing Topical Silver Sulfadiazine and Topical Silver Sulfadiazine–Cerium Nitrate in the Treatment of Moderate and Severe Burns. *Burns* **2001**, *27*, 67–74. [CrossRef] [PubMed]
14. Amin, M.; Glynn, F.; Phelan, S.; Sheahan, P.; Crotty, P.; McShane, D. Silver Nitrate Cauterisation, Does Concentration Matter? *Clin. Otolaryngol.* **2007**, *32*, 197–199.
15. Spacciapoli, P.; Buxton, D.; Rothstein, D.; Friden, P. Antimicrobial Activity of Silver Nitrate against Periodontal Pathogens. *J. Periodontal Res.* **2001**, *36*, 108–113. [CrossRef]
16. Eckhardt, S.; Brunetto, P.S.; Gagnon, J.; Priebe, M.; Giese, B.; Fromm, K.M. Nanobio Silver: Its Interactions with Peptides and Bacteria, and Its Uses in Medicine. *Chem. Rev.* **2013**, *113*, 4708–4754. [CrossRef]
17. Bayston, R.; Vera, L.; Mills, A.; Ashraf, W.; Stevenson, O.; Howdle, S.M. In Vitro Antimicrobial Activity of Silver-Processed Catheters for Neurosurgery. *J. Antimicrob. Chemother.* **2010**, *65*, 258–265. [CrossRef]
18. Fox, C.L.; Modak, S.M. Mechanism of Silver Sulfadiazine Action on Burn Wound Infections. *Antimicrob. Agents Chemother.* **1974**, *5*, 582–588. [CrossRef]
19. Feng, Q.L.; Wu, J.; Chen, G.Q.; Cui, F.Z.; Kim, T.N.; Kim, J.O. A Mechanistic Study of the Antibacterial Effect of Silver Ions on *Escherichia coli* and *Staphylococcus aureus*. *J. Biomed. Mater. Res.* **2000**, *52*, 662–668. [CrossRef]
20. Nomiya, K.; Noguchi, R.; Oda, M. Synthesis and Crystal Structure of Coinage Metal(I) Complexes with Tetrazole (Htetz) and Triphenylphosphine Ligands, and Their Antimicrobial Activities. A Helical Polymer of Silver(I) Complex [Ag(Tetz)(PPh_3)$_2$]$_n$ and a Monomeric Gold(I) Complex [Au(Tetz)(PP]. *Inorg. Chim. Acta* **2000**, *298*, 24–32. [CrossRef]
21. Irisli, S.; Tiryaki, F. Silver (I) Complexes Containing Diphosphine and Bis (Phosphine) Disulphide Ligands. *Asian J. Chem.* **2009**, *21*, 355–360.
22. Sharkey, M.A.; O'Gara, J.P.; Gordon, S.V.; Hackenberg, F.; Healy, C.; Paradisi, F.; Patil, S.; Schaible, B.; Tacke, M. Investigations into the Antibacterial Activity of the Silver-Based Antibiotic Drug Candidate SBC3. *Antibiotics* **2012**, *1*, 25–28. [CrossRef]
23. Carter, K.R.; Miller, R.D.; Hedrick, J.L. Synthesis and Properties of Imide-Aryl Ether 1,2,4-Triazole Random Copolymers. *Polymer* **1993**, *34*, 843–848. [CrossRef]

24. Vatmurge, N.S.; Hazra, B.G.; Pore, V.S.; Shirazi, F.; Chavan, P.S.; Deshpande, M.V. Synthesis and Antimicrobial Activity of β-Lactam–Bile Acid Conjugates Linked via Triazole. *Bioorg. Med. Chem. Lett.* **2008**, *18*, 2043–2047. [CrossRef] [PubMed]
25. Okuno, T.; Oikawa, S.; Goto, T.; Sawai, K.; Shirahama, H.; Matsumoto, T. Structures and Phytotoxicity of Metabolites from Valsa Ceratosperma. *Agric. Biol. Chem.* **2014**, *50*, 997–1001. [CrossRef]
26. Navidpour, L.; Shafaroodi, H.; Abdi, K.; Amini, M.; Ghahremani, M.H.; Dehpour, A.R.; Shafiee, A. Design, Synthesis, and Biological Evaluation of Substituted 3-Alkylthio-4,5-Diaryl-4H-1,2,4-Triazoles as Selective COX-2 Inhibitors. *Bioorg. Med. Chem.* **2006**, *14*, 2507–2517. [CrossRef] [PubMed]
27. Bokor, É.; Docsa, T.; Gergely, P.; Somsák, L. C-Glucopyranosyl-1,2,4-Triazoles as New Potent Inhibitors of Glycogen Phosphorylase. *ACS Med. Chem. Lett.* **2013**, *4*, 612–615. [CrossRef] [PubMed]
28. Blank, B.; Nichols, D.M.; Vaidya, P.D. Synthesis of 1, 2, 4-Triazoles as Potential Hypoglycemic Agents. *J. Med. Chem.* **1972**, *15*, 694–696. [CrossRef]
29. Ainsworth, C.; Easton, N.R.; Livezey, M.; Morrison, D.E.; Gibson, W.R. The Anticonvulsant Activity of 1,2,4-Triazoles. *J. Med. Pharm. Chem.* **1962**, *5*, 383–389. [CrossRef]
30. Radhika, C.; Venkatesham, A.; Sarangapani, M. Synthesis and Antidepressant Activity of Di Substituted-5-Aryl-1,2,4- Triazoles. *Med. Chem. Res.* **2012**, *21*, 3509–3513. [CrossRef]
31. Boechat, N.; Pinheiro, L.C.S.; Santos-Filho, O.A.; Silva, I.C. Design and Synthesis of New N-(5-Trifluoromethyl)-1H-1,2,4-Triazol-3-Yl Benzenesulfonamides as Possible Antimalarial Prototypes. *Molecules* **2011**, *16*, 8083–8097. [CrossRef]
32. Malerich, J.P.; Lam, J.S.; Hart, B.; Fine, R.M.; Klebansky, B.; Tanga, M.J.; D'Andrea, A. Diamino-1,2,4-Triazole Derivatives Are Selective Inhibitors of TYK2 and JAK1 over JAK2 and JAK3. *Bioorg. Med. Chem. Lett.* **2010**, *20*, 7454–7457. [CrossRef] [PubMed]
33. Williamson, D.J.; Hill, R.G.; Shepheard, S.L.; Hargreaves, R.J. The Anti-Migraine 5-HT1B/1D Agonist Rizatriptan Inhibits Neurogenic Dural Vasodilation in Anaesthetized Guinea-Pigs. *Br. J. Pharmacol.* **2001**, *133*, 1029–1034. [CrossRef]
34. Jordão, A.K.; Afonso, P.P.; Ferreira, V.F.; de Souza, M.C.B.V.; Almeida, M.C.B.; Beltrame, C.O.; Paiva, D.P.; Wardell, S.M.S.V.; Wardell, J.L.; Tiekink, E.R.T.; et al. Antiviral Evaluation of N-Amino-1,2,3-Triazoles against Cantagalo Virus Replication in Cell Culture. *Eur. J. Med. Chem.* **2009**, *44*, 3777–3783. [CrossRef]
35. Maletic, M.; Leeman, A.; Szymonifka, M.; Mundt, S.S.; Zokian, H.J.; Shah, K.; Dragovic, J.; Lyons, K.; Thieringer, R.; Vosatka, A.H.; et al. Bicyclo [2.2.2]Octyltriazole Inhibitors of 11β-Hydoxysteroid Dehydrogenase Type 1. Pharmacological Agents for the Treatment of Metabolic Syndrome. *Bioorg. Med. Chem. Lett.* **2011**, *21*, 2568–2572. [CrossRef] [PubMed]
36. Di Mola, N.; Bellasio, E. Potential Antihypertensives. Synthesis of 6-Substituted-N-(4H-1,2,4-Triazol-4-Yl)-3-Pyridazinamines and 3-Substituted-6-(3,5-Dimethyl-1H-1,2,4-Triazol-1-Yl)Pyridazines. *Farmaco. Sci.* **1985**, *40*, 517–533. [CrossRef]
37. Calderone, V.; Giorgi, I.; Livi, O.; Martinotti, E.; Mantuano, E.; Martelli, A.; Nardi, A. Benzoyl and/or Benzyl Substituted 1,2,3-Triazoles as Potassium Channel Activators. VIII. *Eur. J. Med. Chem.* **2005**, *40*, 521–528. [CrossRef]
38. Rodriguez, L.V.; Dedet, J.P.; Paredes, V.; Mendoza, C.; Cardenas, F. A Randomized Trial of Amphotericin B Alone or in Combination with Itraconazole in the Treatment of Mucocutaneous Leishmaniasis. *Mem. Inst. Oswaldo Cruz* **1995**, *90*, 525–528. [CrossRef] [PubMed]
39. Ilango, K.; Valentina, P. Synthesis and Biological Activities of Novel 1,2,4-Triazolo-[3,4-b]-1,3,4-Thiadiazole. *Der Pharma Chem.* **2010**, *2*, 16–22.
40. Jordão, A.K.; Ferreira, V.F.; Lima, E.S.; de Souza, M.C.B.V.; Carlos, E.C.L.; Castro, H.C.; Geraldo, R.B.; Rodrigues, C.R.; Almeida, M.C.B.; Cunha, A.C. Synthesis, Antiplatelet and in Silico Evaluations of Novel N-Substituted-Phenylamino-5-Methyl-1H-1,2,3-Triazole-4-Carbohydrazides. *Bioorg. Med. Chem.* **2009**, *17*, 3713–3719. [CrossRef]
41. Gabryszewski, M.; Wieczorek, B. Silver (I) Complexes with 1, 2, 4-Triazole, 1-Ethyl-1, 2, 4-Triazole, 3-Amino-1, 2, 4-Triazole, 4-Amino-1, 2, 4-Triazole and 3, 5-Diamino-1, 2, 4-Triazole. *Pol. J. Chem.* **1998**, *72*, 2352–2355.
42. Wang, Q.L.; Xu, H.; Hou, H.W.; Yang, G. Synthesis and Structures of Silver(I) Adducts with 4-Amino-4H-1,2,4- Triazole. *Z. Naturforsch. B J. Chem. Sci.* **2009**, *64*, 1143–1146. [CrossRef]
43. Haasnoot, J.G. Mononuclear, Oligonuclear and Polynuclear Metal Coordination Compounds with 1,2,4-Triazole Derivatives as Ligands. *Coord. Chem. Rev.* **2000**, *200–202*, 131–185. [CrossRef]
44. Yi, L.; Ding, B.; Zhao, B.; Cheng, P.; Liao, D.Z.; Yan, S.P.; Jiang, Z.H. Novel Triazole-Bridged Cadmium Coordination Polymers Varying from Zero- to Three-Dimensionality. *Inorg. Chem.* **2004**, *43*, 33–43. [CrossRef] [PubMed]
45. Constable, E.C.; Housecroft, C.E.; Kocik, M.K.; Zampese, J.A. Photoactive Building Blocks for Coordination Complexes: Gilding 2,2′:6′,2″-Terpyridine. *Polyhedron* **2011**, *30*, 2704–2710. [CrossRef]
46. Kang, Y.; Seward, C.; Song, D.; Wang, S. Blue Luminescent Rigid Molecular Rods Bearing N-7-Azaindolyl and 2,2′-Dipyridylamino and Their Zn(II) and Ag(I) Complexes. *Inorg. Chem.* **2003**, *42*, 2789–2797. [CrossRef] [PubMed]
47. Aguado, J.E.; Crespo, O.; Gimeno, M.C.; Jones, P.G.; Laguna, A.; Villacampa, M.D. Coordination Properties of the 1,1′-Bis[((6-Methyl)-2-Pyridyl)Amido]Ferrocene Ligand towards Group 11 Complexes. *Dalton Trans.* **2010**, *39*, 4321–4330. [CrossRef]
48. Al-Mandhary, M.R.A.; Fitchett, C.M.; Steel, P.J.; Al-Mandhary, M.R.A.; Fitchett, C.M.; Steel, P.J. Discrete Metal Complexes of Two Multiply Armed Ligands. *Aust. J. Chem.* **2006**, *59*, 307–314. [CrossRef]
49. Liu, C.S.; Chen, P.Q.; Chang, Z.; Wang, J.J.; Yan, L.F.; Sun, H.W.; Bu, X.H.; Lin, Z.; Li, Z.M.; Batten, S.R. A Photoluminescent Hexanuclear Silver(I) Complex Exhibiting C–H· · · Ag Close Interactions. *Inorg. Chem. Commun.* **2008**, *11*, 159–163. [CrossRef]

50. Zhao, J.; Li, D.S.; Ke, X.J.; Liu, B.; Zou, K.; Hu, H.M. Auxiliary Ligand-Directed Structural Variation from 2D→3D Polythreaded Net to 3-Fold Interpenetrating 3D Pillar-Layered Framework: Syntheses, Crystal Structures and Magnetic Properties. *Dalt. Trans.* **2012**, *41*, 2560–2563. [CrossRef]
51. Hanton, L.R.; Young, A.G. Square-Planar Silver(I)-Containing Polymers Formed from π-Stacked Entities. *Cryst. Growth Des.* **2006**, *6*, 833–835. [CrossRef]
52. Liu, T.F.; Lü, J.; Cao, R. Coordination Polymers Based on Flexible Ditopic Carboxylate or Nitrogen-Donor Ligands. *CrystEngComm* **2010**, *12*, 660–670. [CrossRef]
53. Yoon, I.; Lee, Y.H.; Jung, J.H.; Park, K.M.; Kim, J.; Lee, S.S. Assembly of a Tennis Ball-like Supramolecule Coordinatively Encapsulating Disilver. *Inorg. Chem. Commun.* **2002**, *5*, 820–823. [CrossRef]
54. Njogu, E.M.; Omondi, B.; Nyamori, V.O. Review: Multimetallic Silver(I)–Pyridinyl Complexes: Coordination of Silver(I) and Luminescence. *J. Coord. Chem.* **2015**, *68*, 3389–3431. [CrossRef]
55. Rogovoy, M.I.; Frolova, T.S.; Samsonenko, D.G.; Berezin, A.S.; Bagryanskaya, I.Y.; Nedolya, N.A.; Tarasova, O.A.; Fedin, V.P.; Artem'ev, A.V. 0D to 3D Coordination Assemblies Engineered on Silver(I) Salts and 2-(Alkylsulfanyl)Azine Ligands: Crystal Structures, Dual Luminescence, and Cytotoxic Activity. *Eur. J. Inorg. Chem.* **2020**, *2020*, 1635–1644. [CrossRef]
56. Schmidbaur, H.; Schier, A. Argentophilic Interactions. *Angew. Chem. Int. Ed.* **2015**, *54*, 746–784. [CrossRef]
57. Lippert, B. *Cisplatin: Chemistry and Biochemistry of a Leading Anticancer Drug*; Helvetica Chimica Acta: Zürich, Switzerland, 2006; pp. 1–563. [CrossRef]
58. Adams, M.; Kerby, I.J.; Rocker, I.; Evans, A.; Johansen, K.; Franks, C.R. A Comparison of the Toxicity and Efficacy of Cisplatin and Carboplatin in Advanced Ovarian Cancer. The Swons Gynaecological Cancer Group. *Acta Oncol.* **1989**, *28*, 57–60. [CrossRef]
59. Oun, R.; Moussa, Y.E.; Wheate, N.J. The Side Effects of Platinum-Based Chemotherapy Drugs: A Review for Chemists. *Dalton Trans.* **2018**, *47*, 6645–6653. [CrossRef]
60. Piccart, M.J.; Lamb, H.; Vermorken, J.B. Current and Future Potential Roles of the Platinum Drugs in the Treatment of Ovarian Cancer. *Ann. Oncol. Off. J. Eur. Soc. Med. Oncol.* **2001**, *12*, 1195–1203. [CrossRef]
61. El-Naggar, M.A.; Albering, J.H.; Barakat, A.; Abu-Youssef, M.A.M.; Soliman, S.M.; Badr, A.M.A. New Bioactive 1D Ag(I) Coordination Polymers with Pyrazole and Triazine Ligands; Synthesis, X-Ray Structure, Hirshfeld Analysis and DFT Studies. *Inorg. Chim. Acta* **2022**, *537*, 120948. [CrossRef]
62. Ali, K.A.; Abd-Elzaher, M.M.; Mahmoud, K. Synthesis and Anticancer Properties of Silver(I) Complexes Containing 2,6-Bis(Substituted)Pyridine Derivatives. *Int. J. Med. Chem.* **2013**, *2013*, 256836. [CrossRef] [PubMed]
63. Banti, C.N.; Hadjikakou, S.K. Anti-Proliferative and Anti-Tumor Activity of Silver(i) Compounds. *Metallomics* **2013**, *5*, 569–596.
64. Zaki, M.; Arjmand, F.; Tabassum, S. Current and Future Potential of Metallo Drugs: Revisiting DNA-Binding of Metal Containing Molecules and Their Diverse Mechanism of Action. *Inorg. Chim. Acta* **2016**, *444*, 1–22. [CrossRef]
65. Medici, S.; Peana, M.; Nurchi, V.M.; Lachowicz, J.I.; Crisponi, G.; Zoroddu, M.A. Noble Metals in Medicine: Latest Advances. *Coord. Chem. Rev.* **2015**, *284*, 329–350. [CrossRef]
66. Yousri, A.; Haukka, M.; Abu-Youssef, M.A.M.; Ayoup, M.S.; Ismail, M.M.F.; El Menofy, N.G.; Soliman, S.M.; Barakat, A.; Noa, F.M.A.; Öhrström, L. Synthesis, Structure Diversity, and Antimicrobial Studies of Ag(I) Complexes with Quinoline-Type Ligands. *CrystEngComm* **2023**, *25*, 3922–3930. [CrossRef]
67. El-Naggar, M.A.; Abu-Youssef, M.A.M.; Haukka, M.; Barakat, A.; Sharaf, M.M.; Soliman, S.M. Synthesis, X-ray Structure, and Hirshfeld Analysis of $[Ag(3\text{-amino-}5,6\text{-dimethyl-}1,2,4\text{-triazine})(NO_3)]_n$: A Potent Anticancer and Antimicrobial Agent. *Inorganics* **2023**, *11*, 350. [CrossRef]
68. Rigaku Oxford Diffraction. *CrysAlisPro*; Agilent Technologies Inc.: Oxfordshire, UK, 2020.
69. Sheldrick, G.M. Shelxt–integrated space-group and crystal-structure determination. *Acta Cryst.* **2015**, *A71*, 3–8. [CrossRef]
70. Sheldrick, G.M. Crystal structure refinement with *SHELXL*. *Acta Cryst.* **2015**, *C71*, 3–8.
71. Hübschle, C.B.; Sheldrick, G.M.; Dittrich, B. ShelXle: A Qt graphical user interface for SHELXL. *J. Appl. Cryst.* **2011**, *44*, 1281–1284. [CrossRef]
72. Spackman, M.A.; Jayatilaka, D. Hirshfeld Surface Analysis. *CrystEngComm* **2009**, *11*, 19–32. [CrossRef]
73. Mosmann, T. Rapid Colorimetric Assay for Cellular Growth and Survival: Application to Proliferation and Cytotoxicity Assays. *J. Immunol. Methods* **1983**, *65*, 55–63. [CrossRef] [PubMed]